Complex effective Hamiltonian approach for ir multiphoton dissociation

Thomas M. Flosnik and Robert E. Wyatt
Department of Chemistry and Institute for Theoretical Chemistry, University of Texas at Austin, Austin, Texas 78712-1167
(Received 14 June 1989)

A complex effective Hamiltonian (CEH) approach is formulated in the semiclassical (quantum-molecule–classical-field) representation for the study of ir multiphoton-dissociation processes. This formulation enables one to evaluate the dissociation dynamics in terms of the discrete states only. The effects of the bound–continuum-state interactions are manifested in the CEH matrix by the addition of level shifts and imaginary decay widths to the unperturbed bound-state energies and bound-bound dipole-coupling elements. The periodicity of the CEH matrix in time is preserved, allowing the use of Floquet theory to exactly evaluate the time development of the system. This CEH formulation requires that transitions between continuum states can be safely ignored, that the bound-continuum dipole couplings vary slowly with the continuum state energy ε, and that time t is sufficiently long. High field intensities also tend to make these requirements more stringent. It is found that the CEH matrix in the semiclassical representation can be asymmetric with respect to the level shifts and decay widths. For the ir multiphoton dissociation of a nonrotating model diatomic molecule in the ground electronic state, a rather truncated form of the CEH is tested against a discretized continuum plus optical potential method. Despite the high field intensity and relatively short laser pulse used in these tests, the results indicate that this CEH method works well provided the bound-continuum dipole-coupling elements vary slowly with ε. As can be expected, the validity of the CEH is limited when the bound-continuum dipole couplings vary strongly with ε, which is the case with our model diatomic molecule. The nature of the bound-continuum interactions can apparently have considerable effect on the dissociation dynamics.

I. INTRODUCTION

Multiphoton-excitation (MPE) and dissociation-ionization (MPD-MPI) processes in atoms and molecules continue to generate considerable interest.[1–9] In any theoretical analysis of these phenomena, one is quickly confronted by the problem of how best to account for the field-induced transitions between the unperturbed atomic or molecular states of the discrete (bound) spectrum and those of the continuous (dissociative) spectrum. The interaction of discrete states with one or more continua has been a topic of general interest[10–18] for some time, and is discussed in numerous texts (see, e.g., Refs. 19–21). Methods that use complex, non-Hermitian effective Hamiltonians (CEH) to study such interactions include the Green's or resolvent-operator formulations and various perturbative treatments.[5,22–27] In the CEH method, due to the field-induced interactions between the unperturbed bound states and the continuum, some of the bound-state energies and bound-bound coupling terms of the interaction Hamiltonian will be shifted and acquire imaginary "widths." Those bound states whose energies acquire imaginary widths are commonly known as the "metastable" states of the system. Since the CEH is non-Hermitian, an irreversible loss of probability within the discrete spectrum occurs over time, simulating decay into the continuum.

Although the CEH approach involves some approximations, it does permit one to evaluate the dissociation dynamics in terms of only the bound-state probability amplitudes. Alternative approaches include the various L^2 discretized continuum schemes such as dilatation transformations,[5,28–31] R matrix,[32,33] and the discretized continuum plus optical potential method.[34–36] Although these methods are, in principle, accurate, they can be rendered impractical by the huge number of discrete pseudocontinuum states that may be required. The various finite-difference methods[34,37–39] are also possible alternatives, and can be used to evaluate fragment momentum distribution, etc. However, these calculations become prohibitive for longer times and for molecules much larger than diatomics. Hence, a better understanding of the CEH approach may be useful.

In this work, we will use the CEH approach to study the collisionless infrared (ir) MPD of a model, nonrotating, diatomic molecule in the ground electronic state. The CEH approach used here will be formulated in the semiclassical (quantum-molecule–classical-field) representation. This system will enable us to directly compare our CEH results with the BOXSW (discretized continuum plus optical potential) method of Leforestier and Wyatt.[34–36] The model diatomic molecule is based on a modified[34] Stine-Noid[40] hydrogen fluoride (HF) molecular potential $V(r)$ and dipole function $\mu(r)$, which are described in Table I. The relative energies of the $N=6$ bound states $\chi_n(r)$ $(n=0,1,\ldots,5)$ for this molecule are shown in Table II. This model should be of some general interest, since the dipole functions[41,42] and infrared MPE-MPD dynamics of the HF molecule have been studied extensively in the past.[32,34,39,40,43–55] Over a time interval of ten field periods, at a field frequency and intensity of 2880 cm^{-1} and 10^{14} W/cm^2, respectively, Lefores-

TABLE I. Description of the diatomic molecule and the Saxon-Wood potential.

A. Molecular Hamiltonian	
$H^0=(-\hbar^2/2m)d^2/dr^2+V(r)$	$m=1731.7$ a.u.
$V(r)=D\{\exp[-\alpha(r-r_e)]-1\}^2-D$	$D=6.16624\times10^{-2}$ aeu
	$\alpha=2.25173$ a.u.
	$r_e=1.75$ a.u.
	$\hbar=1$ aeu,atu
B. Dipole function	
$\mu(r)=Ar[\exp(-\xi r^4)]$	$A=0.4541$ a.u.
	$\xi=0.02665$ a.u.
C. Saxon-Wood potential	
$W(r)=-iV_0\{1+\exp[(r^*-r)/\gamma]\}^{-1}$	$V_0=0.02$ aeu
	$\gamma=0.35$ a.u.
	$r^*=7.0$ a.u.

tier and Wyatt obtained excellent agreement when they compared BOXSW dissociation probabilities for this system with those from a finite-difference calculation.[34] We will derive our CEH quantum equations of motion in Sec. II. In doing so, particular attention will be given to the validity of the approximations made, and their effects on the MPD dynamics. Our final CEH matrix will be periodic in time, and curiously enough, asymmetric with respect to the shifts and widths resulting from the bound-continuum interactions. We will discuss the origin of this seemingly anomalous result later in some detail. In Sec. III, we will perform some numerical calculations comparing the CEH and BOXSW methods.

Aside from enabling us to compare the CEH and BOXSW methods, the semiclassical representation was also chosen for the following reasons. In this representation the field can be treated as a time-dependent driving term in the total Hamiltonian $H(r,t)$, which allows one to expand the time-dependent wave function $\Psi(r,t)$ in terms of the molecular eigenstates only, rather than a combined molecule-field basis such as in the full quantum representation. Also, by representing the field as a monochromatic, linearly polarized laser of constant electric field amplitude E^0 and frequency ω, such that $H(r,t)$ is periodic [i.e., $H(r,t)=H(r,t+\tau)$ where $\tau=2\pi/\omega$], we can use Floquet theory (see, e.g., Refs. 5, 34–36, 43–47, and 56–66) to calculate exact long-time solutions for $\Psi(r,t)$ without resorting to the rotating-wave approximation.[66,67] The Floquet theory exploits the periodicity of $H(r,t)$, so that one can use the time propagator $U(t)$, evaluated over the first full (or half) period of the field,[46] to obtain $\Psi(r,t)$ at long time.

TABLE II. Continuum threshold energy and *relative* energies of the bound molecular states.

$\varepsilon_{\text{threshold}}=11\,528\ \text{cm}^{-1}$
$\varepsilon_5=11\,213\ \text{cm}^{-1}$
$\varepsilon_4=10\,256\ \text{cm}^{-1}$
$\varepsilon_3=8655\ \text{cm}^{-1}$
$\varepsilon_2=6413\ \text{cm}^{-1}$
$\varepsilon_1=3528\ \text{cm}^{-1}$
$\varepsilon_0=0\ \text{cm}^{-1}$

As we will be comparing the CEH and BOXSW methods for our model diatomic molecule, a brief description of the BOXSW method is in order.[34–36] In this method, an infinite potential barrier is erected at a sufficiently large internuclear distance r^*, where $V(r)$ is effectively zero, so that the bound molecular states, and a sufficiently dense set of discretized pseudocontinuum states, can be expanded in terms of a convenient L^2 basis such as sine functions. This pseudocontinuum is not truly dissipative, since any probability in these states will eventually be reflected by the infinite barrier at r^*, producing incorrect and artificial feedback with the bound states.[34] To prevent this artificial feedback, a complex Saxon-Wood optical potential $W(r)$,[34–36,49,50] described in Table I, is introduced near r^* to smoothly damp the pseudocontinuum probabilities at the barrier. The BOXSW parameters V_0,γ, and the barrier location r^* are chosen so that when the complete unperturbed molecular Hamiltonian $H^0(r)$ *plus* the optical potential $W(r)$ are diagonalized in the L^2 basis, the unperturbed bound molecular eigenstates and eigenvalues will be only negligibly affected by $W(r)$, but the eigenvalues of the pseudocontinuum states will acquire a negative, imaginary "width" to ensure smooth damping of their probabilities at the barrier. Once a converged calculation for the BOXSW is achieved, it has been found[34–36] that the transition and dissociation probabilities are not overly sensitive to reasonable variations in the optical potential parameters, provided r^* is large enough to ensure that $W(r)$ will not significantly affect the bound molecular states. In some sense, within the interval ($r=0$, $r=r^*$) at energy ε, a pseudocontinuum state mimics a true continuum state $\chi(\varepsilon,r)$, for which $\chi(\varepsilon,r^*)=0$.[36] Although the energies of the metastable molecular states in CEH methods also have a negative imaginary width, the physical origin of these widths is different. In the BOXSW, the bound-state energies have only negligibly small widths due to the complex potential $W(r)$, which can be ignored. Dissocation occurs via transitions from the bound states into the pseudocontinuum states, whose probabilities are then smoothly damped via $W(r)$. In the CEH formulation, the energies of some bound states acquire non-negligible imaginary widths as a result of field-induced interactions with the dissociative continuum.

II. THE "EFFECTIVE" QUANTUM EQUATIONS OF MOTION

The following derivation is similar in spirit to the approach of Cohen-Tannoudji, Diu, and Laloe,[19] who treat the decay of a *single* discrete state into the continuum by means of a time-*independent* perturbation. The system considered here consists of a nonrotating, quantum Morse oscillator, whose bound states are coupled to each other and the dissociative continuum via a classical, monochromatic, linearly polarized laser. The total Hamiltonian $H(r,t)$ is

$$H(r,t)=H^0(r)-E^0\mu(r)\cos\omega t \ . \tag{1}$$

We will denote the bound states $\chi_n(r)$ as $|n\rangle$, and the continuum states $\chi(\varepsilon,r)$ as $|\varepsilon\rangle$, The molecular states satisfy the following relations:

$$H^0|n\rangle=\varepsilon_n|n\rangle, \quad \text{where } \varepsilon_n<0 \tag{2a}$$

$$H^0|\varepsilon\rangle=\varepsilon|\varepsilon\rangle, \quad \text{where } \varepsilon>0 \tag{2b}$$

$$\langle m|n\rangle=\delta_{mn} \ , \tag{2c}$$

$$\langle \varepsilon'|\varepsilon\rangle=\delta(\varepsilon'-\varepsilon) \ , \tag{2d}$$

$$\langle \varepsilon|n\rangle=0 \ , \tag{2e}$$

and

$$\sum_{n=0}^{n=5}|n\rangle\langle n|+\int_0^\infty d\varepsilon\,|\varepsilon\rangle\langle\varepsilon|=\hat{1} \ . \tag{2f}$$

In the interaction picture, the time-dependent wave function is expressed as

$$\Psi^I(r,t)=\sum_{n=0}^{n=5}b_n(t)e^{-i\omega_n t}|n\rangle + \int_0^\infty d\varepsilon\, b(\varepsilon,t)e^{-i\omega_\varepsilon t}|\varepsilon\rangle \ , \tag{3}$$

with

$$\sum_{n=0}^{n=5}|b_n(t)|^2+\int_0^\infty d\varepsilon\,|b(\varepsilon,t)|^2=1 \ , \tag{4}$$

where $\varepsilon_n=\hbar\omega_n$ and $\varepsilon=\hbar\omega_\varepsilon$. The probability of occupying the bound state $|n\rangle$ at time t is $|b_n(t)|^2$, and the probability of occupying a continuum state $|\varepsilon\rangle$ at time t in the energy interval $(\varepsilon,\varepsilon+d\varepsilon)$ is given by $|b(\varepsilon,t)|^2d\varepsilon$. Substituting Eq. (3) into the time-dependent Schrödinger equation, and projecting onto the stationary states $e^{-i\omega_n t}|n\rangle$, etc., yields the following infinite set of coupled, first-order differential equations:

$$i\hbar\dot{b}_n(t)=-\sum_{m=0}^{m=5}b_m(t)V_{nm}\cos(\omega t)e^{i\omega_{nm}t} - \int_0^\infty d\varepsilon\, b(\varepsilon,t)V_{n\varepsilon}\cos(\omega t)e^{i\omega_{n\varepsilon}t} \ , \tag{5}$$

$$i\hbar\dot{b}(\varepsilon,t)=-\sum_{m=0}^{m=5}b_m(t)V_{\varepsilon m}\cos(\omega t)e^{i\omega_{\varepsilon m}t} - \int_0^\infty d\varepsilon' b(\varepsilon',t)V_{\varepsilon\varepsilon'}\cos(\omega t)e^{i\omega_{\varepsilon\varepsilon'}t} \ , \tag{6}$$

where $V_{\varepsilon m}=E^0\langle\varepsilon|\mu(r)|m\rangle$ and $\omega_{\varepsilon m}=\omega_\varepsilon-\omega_m$, etc.

Our first approximation consists of neglecting terms in Eqs. (6) that contain the elements $V_{\varepsilon\varepsilon'}$ which couple the continuum states $|\varepsilon'\rangle$ and $|\varepsilon\rangle$. Since $\mu(r)$ decreases rapidly for $r>r_e$, we will assume that the dissociating molecule separates too quickly, relative to the photon absorption rate, for transitions between continuum states to be of much importance. The validity of this approximation will depend of course on the field strength and the distance over which $\mu(r)$ can effectively couple any given pair of continuum states. The BOXSW (Ref. 34) was used to test this approximation at $\omega=2880$ cm^{-1} by "turning off" the coupling elements between the pseudocontinuum states. The resulting dissociation probabilities from the uppermost ($n=5$) bound state were then compared, for intensities I of 10^{14} and 10^{12} W/cm^2, with the exact probabilities in which the full values of all coupling elements were retained. Floquet theory was used to evaluate the time development of the system. The time propagator matrix $\underline{U}(t)$ (see Refs. 34–36, 43–46, and 61) was obtained over the first field period τ by means of a Bulirsch-Stoer numerical integrator using 64 time steps. The dissociation probabilities at $I=10^{14}$ W/cm^2 were appreciably affected ($\sim$20–30 %) by the couplings between pseudocontinuum states, whereas those at $I=10^{12}$ W/cm^2 were not. It would thus seem reasonable to infer that continuum-continuum transitions in this case can be safely neglected, except perhaps at the very highest laser intensities (at a field intensity of 10^{14} W/cm^2 a real diatomic molecule would probably undergo dielectric breakdown or a change in dipole, etc.[68]).

For reasonable field strengths, we will approximate Eqs. (6) as

$$i\hbar\dot{b}(\varepsilon,t)\cong-\sum_{m=0}^{m=5}b_m(t)V_{\varepsilon m}\cos(\omega t)e^{i\omega_{\varepsilon m}t} \ . \tag{7}$$

The formal solution for Eqs. (7), in which $b(\varepsilon,t=0)=0$, is written as

$$b(\varepsilon,t)\cong-(1/i\hbar)\sum_{m=0}^{m=5}\int_0^t dt' b_m(t')V_{\varepsilon m} \times\cos(\omega t')e^{i\omega_{\varepsilon m}t'} \ . \tag{8}$$

Substituting Eqs. (8) into Eqs. (5) allows the infinite set of coupled differential equations to be reduced to the following finite (i.e., N)-dimensional set of integro-differential equations:

$$i\hbar\dot{b}_n(t)\cong-\sum_{m=0}^{m=5}b_m(t)V_{nm}\cos(\omega t)e^{i\omega_{nm}t} +(1/i\hbar)\sum_{m=0}^{m=5}\int_0^\infty d\varepsilon\int_0^t dt' b_m(t')V_{n\varepsilon}V_{\varepsilon m}e^{i\omega_\varepsilon(t'-t)}e^{-i\omega_m t'}\cos(\omega t')e^{i\omega_n t}\cos(\omega t) \ . \tag{9}$$

At this point one might wonder under what circumstances, if any, can Eqs. (9) be simplified by replacing the probability amplitudes $b_m(t')$ with $b_m(t)$. In other words, when does the system have a sufficiently short memory such that the only values of t' we need to worry about are those for which $b_m(t') \sim b_m(t)$? By integrating Eqs. (9) over ε first, we can try to determine when the contributions of the resulting integrand in t' will diminish rapidly, *except* for those values of t' where $b_m(t') \sim b_m(t)$.

The integral over ε in Eqs. (9) will be approximated with a sum of integrals, by assuming that the quantities $V_{\varepsilon m}$, etc., are effectively constant over a series of energy intervals $[\varepsilon_j, \varepsilon_j + \Delta\varepsilon_j]$, where $\Delta\varepsilon_j$ can be adjusted in order to maintain some arbitrary degree of accuracy. The size of each interval obviously depends on the behavior of the bound-continuum couplings in the vicinity of ε_j. By considering only a single term in the summation over bound states $|m\rangle$ (remembering that $\varepsilon = \hbar\omega_\varepsilon$, $\varepsilon_{j+1} = \varepsilon_j + \Delta\varepsilon_j$, and $\varepsilon_{j=0} = 0$), we have the relation

$$\int_0^\infty d\varepsilon\, V_{n\varepsilon} V_{\varepsilon m} e^{i\omega_\varepsilon (t'-t)} \cong \sum_{j=0}^{\infty} V_{n\varepsilon_j} V_{\varepsilon_j m} \int_{\varepsilon_j}^{\varepsilon_j + \Delta\varepsilon_j} d\varepsilon\, e^{i\varepsilon(t'-t)/\hbar} . \quad (10)$$

Evaluating the integral on the right-hand side (RHS) of Eq. (10) yields

$$\int_0^\infty d\varepsilon\, V_{n\varepsilon} V_{\varepsilon m} e^{i\omega_\varepsilon (t'-t)} \cong \sum_{j=0}^{\infty} V_{n\varepsilon_j} V_{\varepsilon_j m} [-i\hbar/(t'-t)] \times (e^{i(\varepsilon_j + \Delta\varepsilon_j)(t'-t)/\hbar} - e^{i\varepsilon_j (t'-t)/\hbar}) . \quad (11)$$

After rewriting the exponentials on the RHS of Eq. (11) we have

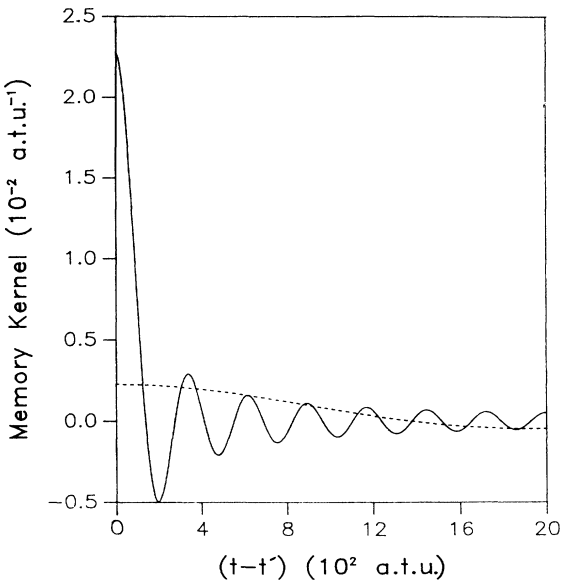

FIG. 1. The memory kernel $g_j(t'-t)$ vs $(t-t')$ for $\Delta\varepsilon_j = 1000$ cm^{-1} (— — —) and 10 000 cm^{-1} (——).

$$\int_0^\infty d\varepsilon\, V_{n\varepsilon} V_{\varepsilon m} e^{i\omega_\varepsilon (t'-t)} \cong \sum_{j=0}^{\infty} V_{n\varepsilon_j} V_{\varepsilon_j m} [2\hbar/(t'-t)] \times \{\sin[\Delta\varepsilon_j (t'-t)/2\hbar]\} e^{i\Theta_j (t'-t)} , \quad (12)$$

where $\Theta_j = (2\varepsilon_j + \Delta\varepsilon_j)/2\hbar$. We will identify the quantity $\{\sin[\Delta\varepsilon_j (t'-t)/2\hbar]\}/(t'-t)$ on the RHS of Eq. (12) as the memory kernel $g_j(t'-t)$. Examples of the memory kernel are shown in Fig. 1 for two values of $\Delta\varepsilon_j$. Substituting Eq. (12) into Eqs. (9) and collecting terms yields

$$i\hbar \dot{b}_n(t) \cong -\sum_{m=0}^{m=5} b_m(t) V_{nm} \cos(\omega t) e^{i\omega_{nm} t} + (2/i) \sum_{m=0}^{m=5} \sum_{j=0}^{\infty} V_{n\varepsilon_j} V_{\varepsilon_j m} e^{i\omega_n t} \cos(\omega t) \int_0^t dt' b_m(t') g_j(t'-t) e^{i\Theta_j (t'-t)} e^{-i\omega_m t'} \cos(\omega t') . \quad (13)$$

If the bound-continuum couplings vary slowly with ε, we can select larger intervals $\Delta\varepsilon_j$ and still retain some given degree of accuracy. As the quantity $(\Delta\varepsilon_j/2\hbar)$ becomes very large relative to $(t'-t)$ we can apply the well-known result

$$\lim_{L\to\infty} (\sin Lx)/x = \pi\delta(x) \quad (14)$$

to the memory kernel $g_j(t'-t)$, such that

$$\lim_{\Delta\varepsilon_j \to \infty} g_j(t'-t) = \pi\delta(t'-t) . \quad (15)$$

Therefore, as the bound-continuum couplings vary more slowly with ε, the system's "memory" of previous events in the integral over t' shortens, such that only those times t' immediately prior to t are important. However, full convergence of $g_j(t'-t)$ to $\pi\delta(t'-t)$ is not physically reasonable, nor is it necessary. If the contributions to the integral over t' in Eqs. (9) and (13) are negligible, *except* for those values of t' which satisfy the condition $b_m(t') \sim b_m(t)$, then $b_m(t')$ can be approximately replaced with $b_m(t)$ and factored out of the integral over t'. Since the global maximum in $g_j(t'-t)$, is at $t'=t$, and the first point where $g_j(t'-t)$ is zero occurs at $|(t'-t)| = 2\pi\hbar/\Delta\varepsilon_j$, the interval $[t'=2\pi\hbar/\Delta\varepsilon_j, t'=t]$ contains the region in which $g_j(t'-t)$ is most strongly peaked, and $g_j(t'-t)$ diminishes rapidly for $|(t'-t)| \gg 2\pi\hbar/\Delta\varepsilon_j$. Therefore, in order that $g_j(t'-t)$ behave as a δ function relative to $b_m(t')$, it is necessary that the condition $b_m(t') \sim b_m(t)$ holds over an interval $[t', t'=t]$ much larger than the quantity $2\pi\hbar/\Delta\varepsilon_j$. This

"δ-function" behavior of the memory kernel relative to $b_m(t')$ rests on the combination of two factors, the energy dependence of the bound-continuum couplings and the rate of change in the amplitudes $b_m(t')$, which in turn depends on the field strength. As the intensity I increases, the probability amplitudes oscillate more rapidly in time, and the bound-continuum couplings must vary more slowly with ε in order that the memory kernel behave as a δ function relative to the probability amplitudes.

By approximately replacing $b_m(t')$ with $b_m(t)$ in Eqs. (9) we have

$$i\hbar\dot{b}_n(t)\cong-\sum_{m=0}^{m=5}b_m(t)V_{nm}\cos(\omega t)e^{i\omega_{nm}t}+(1/2i\hbar)\sum_{m=0}^{m=5}\int_0^\infty d\varepsilon\, V_{n\varepsilon}V_{\varepsilon m}b_m(t)\cos(\omega t)e^{i\omega_n t}\int_0^t dt' e^{i\omega_\varepsilon(t'-t)}e^{-i(\omega_m-\omega)t'}$$
$$+(1/2i\hbar)\sum_{m=0}^{m=5}\int_0^\infty d\varepsilon\, V_{n\varepsilon}V_{\varepsilon m}b_m(t)\cos(\omega t)e^{i\omega_n t}\int_0^t dt' e^{i\omega_\varepsilon(t'-t)}e^{-i(\omega_m+\omega)t'}\ . \tag{16}$$

Multiplying the integrands in t' by the appropriate factors $e^{i(\omega_m\pm\omega)t}$ and their respective complex conjugates, and defining $\tau'=(t-t')$, Eqs. (16) become

$$i\hbar\dot{b}_n(t)\cong-\sum_{m=0}^{m=5}b_m(t)V_{nm}\cos(\omega t)e^{i\omega_{nm}t}+(1/2i\hbar)\sum_{m=0}^{m=5}\int_0^\infty d\varepsilon\, V_{n\varepsilon}V_{\varepsilon m}b_m(t)\cos(\omega t)e^{i\omega_{nm}t}e^{i\omega t}\int_0^t d\tau' e^{-i(\omega_\varepsilon-\omega_m+\omega)\tau'}$$
$$+(1/2i\hbar)\sum_{m=0}^{m=5}\int_0^\infty d\varepsilon\, V_{n\varepsilon}V_{\varepsilon m}b_m(t)\cos(\omega t)e^{i\omega_{nm}t}e^{-i\omega t}\int_0^t d\tau' e^{-i(\omega_\varepsilon-\omega_m-\omega)\tau'}\ . \tag{17}$$

Evaluating the integrals over τ' yields

$$\int_0^t d\tau' e^{-i(\varepsilon-\varepsilon_m\pm\hbar\omega)\tau'/\hbar}=\hbar[G_m(\varepsilon,\pm\hbar\omega)-iD_m(\varepsilon,\pm\hbar\omega)]\ , \tag{18}$$

where

$$D_m(\varepsilon,\pm\hbar\omega)=\{1-\cos[(\varepsilon-\varepsilon_m\pm\hbar\omega)t/\hbar]\}/(\varepsilon-\varepsilon_m\pm\hbar\omega)\ , \tag{19a}$$

$$G_m(\varepsilon,\pm\hbar\omega)=\{\sin[(\varepsilon-\varepsilon_m\pm\hbar\omega)t/\hbar]\}/(\varepsilon-\varepsilon_m\pm\hbar\omega)\ . \tag{19b}$$

Substituting Eqs. (18) into Eqs. (17) yields

$$i\hbar\dot{b}_n(t)\cong-\sum_{m=0}^{m=5}b_m(t)V_{nm}\cos(\omega t)e^{i\omega_{nm}t}-\tfrac{1}{2}\sum_{m=0}^{m=5}b_m(t)\cos(\omega t)e^{i\omega_{nm}t}e^{i\omega t}\int_0^\infty d\varepsilon\, V_{n\varepsilon}V_{\varepsilon m}D_m(\varepsilon,+\hbar\omega)$$
$$-(i/2)\sum_{m=0}^{m=5}b_m(t)\cos(\omega t)e^{i\omega_{nm}t}e^{i\omega t}\int_0^\infty d\varepsilon\, V_{n\varepsilon}V_{\varepsilon m}G_m(\varepsilon,+\hbar\omega)$$
$$-\tfrac{1}{2}\sum_{m=0}^{m=5}b_m(t)\cos(\omega t)e^{i\omega_{nm}t}e^{-i\omega t}\mathrm{P}\int_0^\infty d\varepsilon\, V_{n\varepsilon}V_{\varepsilon m}D_m(\varepsilon,-\hbar\omega)$$
$$-(i/2)\sum_{m=0}^{m=5}b_m(t)\cos(\omega t)e^{i\omega_{nm}t}e^{-i\omega t}\int_0^\infty d\varepsilon\, V_{n\varepsilon}V_{\varepsilon m}G_m(\varepsilon,-\hbar\omega)\ , \tag{20}$$

where P indicates taking the principle value of the integral, when necessary.

It should be noted that the factors $G_m(\varepsilon,\pm\hbar\omega)$ are of the form $[\sin a(x\text{-}x_0)]/(x-x_0)$, reminiscent of Eqs. (14) and (15), where $x=\varepsilon$, $a=t/\hbar$, and $x_0=\varepsilon_m\pm\hbar\omega$. At very long time t, Eq. (19b) converges to δ functions

$$\lim_{t\to\infty}G_m(\varepsilon,\pm\hbar\omega)=\pi\delta(\varepsilon-\varepsilon_m\pm\hbar\omega)\ . \tag{21}$$

Just what "very long time" means in this context can be estimated by examining the behavior of the functions $G_m(\varepsilon,\pm\hbar\omega)$ in conjunction with the relation

$$\int_{-\infty}^{\infty}d(x-x_0)\{[\sin a(x-x_0)]/(x-x_0)\}=\pi\ . \tag{22}$$

At any given time t, the functions $G_m(\varepsilon,\pm\hbar\omega)$ will have global maxima at $\varepsilon=\varepsilon_m-\hbar\omega$ and $\varepsilon=\varepsilon_m+\hbar\omega$ (i.e., $x=x_0$), respectively, where the "height" of this maximum is $t/\hbar$ (i.e., a). The "base width" for the positive portion of this "spike" and the period of oscillation for the "wings" on either side of this "spike" is $2\pi\hbar/t$. As the height $t/\hbar$ becomes large and the base width $2\pi\hbar/t$ narrows, these "spikes" in $G_m(\varepsilon,\pm\hbar\omega)$ can be approximated by isosceles triangles having area π. This is illustrated in Fig. 2 where $G_m(\varepsilon,\pm\hbar\omega)$ is shown for times $t=0.5\times10^5$ atu (atomic time units) and 2.0×10^5 atu. Therefore, as t increases these positive "spikes" in the functions $G_m(\varepsilon,\pm\hbar\omega)$ are responsible for nearly the entire net value of the integral in Eq. (22).

As defined previously we have $\varepsilon_m<0$ for all $|m\rangle$; therefore the maximum in $G_m(\varepsilon,+\hbar\omega)$ occurs at

$\varepsilon=\varepsilon_m-\hbar\omega$, which lies *outside* the limits of integration over ε in Eqs. (20). If t is long enough so that the base of the "spike" in $G_m(\varepsilon,+\hbar\omega)$ no longer extends into the region $\varepsilon>0$, and if the bound-continuum couplings vary slowly with ε relative to the oscillating wings of $G_m(\varepsilon,+\hbar\omega)$, then the integrals in Eqs. (20) containing $G_m(\varepsilon,+\hbar\omega)$ will become negligible. Since the base width of this "spike" is $2\pi\hbar/t$, the "spike" in $G_m(\varepsilon,+\hbar\omega)$ will no longer extend into the positive ε axis when $\varepsilon=\varepsilon_m-\hbar\omega+\pi\hbar/t<0$. Similarly, for bound states $|m\rangle$, where $\varepsilon=\varepsilon_m+\hbar\omega+\pi\hbar/t<0$, the integrals in $G_m(\varepsilon,-\hbar\omega)$ will also become negligible at long t. For bound states $|m\rangle$, where $\varepsilon_m+\hbar\omega>0$ (i.e., those bound states $|m\rangle$ which can make energy-conserving transitions into the continuum by absorbing a single photon of frequency ω), the integrals in $G_m(\varepsilon,-\hbar\omega)$ will have non-negligible values. For these states it can be argued that $G_m(\varepsilon,-\hbar\omega)$ behaves as a δ function *relative* to $V_{n\varepsilon}$ and $V_{\varepsilon m}$ when these couplings are approximately constant over an energy interval of width $\Delta\varepsilon$, centered at $\varepsilon=\varepsilon_m+\hbar\omega$, where $\Delta\varepsilon\gg 2\pi\hbar/t$. After evaluating $V_{n\varepsilon}$ and $V_{\varepsilon m}$ at $\varepsilon=\varepsilon_m+\hbar\omega$ and factoring them out of the integral over ε, the lower limit of integration can be safely extended to $-\infty$ as in Eq. (22). Under the appropriate conditions we have the following results:

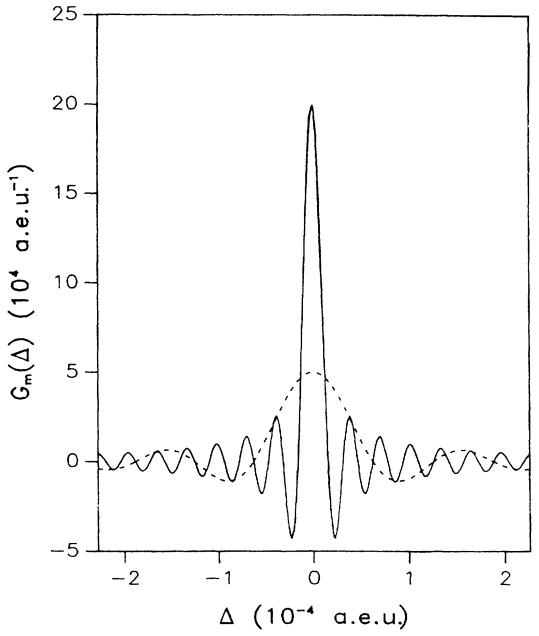

FIG. 2. $G_m(\Delta)$ vs Δ, where $\Delta=\varepsilon-\varepsilon_m\pm\hbar\omega$, for $t=0.5\times10^5$ atu (— — —) and 2.0×10^5 atu (——).

$$\int_0^\infty d\varepsilon\, V_{n\varepsilon}V_{\varepsilon m}G_m(\varepsilon,+\hbar\omega)\sim 0 \quad \text{when } \varepsilon=\varepsilon_m-\hbar\omega+\pi\hbar/t<0 \text{ and } t\gg 2\pi\hbar/\Delta\varepsilon\ , \tag{23a}$$

$$\int_0^\infty d\varepsilon\, V_{n\varepsilon}V_{\varepsilon m}G_m(\varepsilon,-\hbar\omega)\sim \begin{cases} 0 \text{ when } \varepsilon=\varepsilon_m+\hbar\omega+\pi\hbar/t<0 \text{ and } t\gg 2\pi\hbar/\Delta\varepsilon\ , \\ \pi V_{n\varepsilon}V_{\varepsilon m}(\varepsilon=\varepsilon_m+\hbar\omega>0) \quad \text{for } t\gg 2\pi\hbar/\Delta\varepsilon\ . \end{cases} \tag{23b}$$

Defining $\pi V_{n\varepsilon}V_{\varepsilon m}(\varepsilon=\varepsilon_m+\hbar\omega>0)$ as $\Gamma_{nm}(\varepsilon=\varepsilon_m+\hbar\omega>0)$ and using Eqs. (23), Eqs. (20) at sufficiently long time t are written as

$$i\hbar\dot{b}_n(t)\cong-\sum_{m=0}^{m=5}b_m(t)\cos(\omega t)e^{i\omega_{nm}t}\left[V_{nm}+\tfrac{1}{2}\mathrm{P}\int_0^\infty d\varepsilon\, V_{n\varepsilon}V_{\varepsilon m}[e^{i\omega t}D_m(\varepsilon,+\hbar\omega)+e^{-i\omega t}D_m(\varepsilon,-\hbar\omega)]\right.$$
$$\left.+(ie^{-i\omega t}/2)\Gamma_{nm}(\varepsilon=\varepsilon_m+\hbar\omega>0)\right]\ . \tag{24}$$

Transforming to the Schrödinger picture where $b_n^s(t)=e^{-i\varepsilon_n t/\hbar}b_n(t)$, Eqs. (24) in matrix form are written as

$$i\hbar\underline{\dot{b}}^{\,s}(t)\cong\underline{H}^s(r,t)\underline{b}^s(t)\ , \tag{25}$$

where the elements of the CEH matrix $\underline{H}^s(r,t)$ are

$$[\underline{H}^s(r,t)]_{n,n}=\varepsilon_n-\cos(\omega t)\left[V_{nn}+\tfrac{1}{2}\mathrm{P}\int_0^\infty d\varepsilon\,|V_{n\varepsilon}|^2[e^{i\omega t}D_n(\varepsilon,+\hbar\omega)+e^{-i\omega t}D_n(\varepsilon,-\hbar\omega)]\right.$$
$$\left.+(ie^{-i\omega t}/2)\Gamma_{nn}(\varepsilon=\varepsilon_n+\hbar\omega>0)\right]\ , \tag{26a}$$

$$[\underline{H}^s(r,t)]_{n,m\neq n}=-\cos(\omega t)\left[V_{nm}+\tfrac{1}{2}\mathrm{P}\int_0^\infty d\varepsilon\, V_{n\varepsilon}V_{\varepsilon m}[e^{i\omega t}D_m(\varepsilon,+\hbar\omega)+e^{-i\omega t}D_m(\varepsilon,-\hbar\omega)]\right.$$
$$\left.+(ie^{-i\omega t}/2)\Gamma_{nm}(\varepsilon=\varepsilon_m+\hbar\omega>0)\right]\ , \tag{26b}$$

$$[\underline{H}^s(r,t)]_{m,n\neq m}=-\cos(\omega t)\left[V_{mn}+\tfrac{1}{2}\mathrm{P}\int_0^\infty d\varepsilon\, V_{m\varepsilon}V_{\varepsilon n}[e^{i\omega t}D_n(\varepsilon,+\hbar\omega)+e^{-i\omega t}D_n(\varepsilon,-\hbar\omega)]\right.$$
$$\left.+(ie^{-i\omega t}/2)\Gamma_{mn}(\varepsilon=\varepsilon_n+\hbar\omega>0)\right]\ . \tag{26c}$$

The terms in Eqs. (26) can be easily identified as follows. On the diagonal, the term V_{nn} is just the first-order perturbative correction to ε_n. The integral over ε containing the factors $D_n(\varepsilon,\pm\hbar\omega)$ in (26a) is the *level shift*, induced in ε_n to second order by the interactions between the bound state $|n\rangle$ and the continuum states $|\varepsilon\rangle$. The complex term containing $\Gamma_{nn}(\varepsilon=\varepsilon_n+\hbar\omega>0)$ is the *decay width* of the "metastable" discrete state $|n\rangle$. The metastable states in this formulation are those bound states which are energetically within one photon of the dissociative continuum. The off-diagonal level shifts and widths in Eqs. (26b) and (26c) are due to interactions between bound states $|n\rangle$ and $|m\rangle$ by means of their mutual coupling with the continuum.[5,25] These off-diagonal shifts and widths are well known,[5,22–26] and may lead to various interference effects.[22,25,26] In Sec. III, we will briefly examine how these off-diagonal widths affect the time-dependent dissocation profiles.

Although the CEH matrix $\underline{H}^s(r,t)$ has the proper periodicity in order to apply the Floquet theory, it is also obvious from Eqs. (24) and (26) that $\underline{H}^s(r,t)$ will, unless $\varepsilon_n=\varepsilon_m$ for all n and m, be *asymmetric with respect to the level shifts and widths.* For the off-diagonal level shifts, this asymmetry is due to the differences between $D_n(\varepsilon,\pm\hbar\omega)$ and $D_m(\varepsilon,\pm\hbar\omega)$. Note that the off-diagonal decay widths $\Gamma_{mn}(\varepsilon=\varepsilon_n+\hbar\omega>0)$ and $\Gamma_{nm}(\varepsilon=\varepsilon_m+\hbar\omega>0)$ are nonzero at long time *only* for those states $|n\rangle$ and $|m\rangle$ where $\varepsilon_n+\hbar\omega>0$ and $\varepsilon_m+\hbar\omega>0$. If we have $\varepsilon_m+\hbar\omega>0$ *but* $\varepsilon_n+\hbar\omega<0$, then $\Gamma_{mn}(\varepsilon=\varepsilon_n+\hbar\omega>0)$ will be zero, whereas $\Gamma_{nm}(\varepsilon=\varepsilon_m+\hbar\omega>0)$ will *not*, which leads to an obvious asymmetry in $\underline{H}^s(r,t)$. Even in the case where $|n\rangle$ and $|m\rangle$ are both energetically within one photon of the continuum, there remains the possibility that $V_{n\varepsilon}$ and $V_{\varepsilon m}$ will vary strongly enough at the energies $\varepsilon=\varepsilon_n+\hbar\omega$ and $\varepsilon=\varepsilon_m+\hbar\omega$, such that $\Gamma_{mn}(\varepsilon=\varepsilon_n+\hbar\omega>0)\neq\Gamma_{nm}(\varepsilon=\varepsilon_m+\hbar\omega>0)$. This condition may also signal a breakdown in other approximations, such as replacing $b_m(t')$ by $b_m(t)$ in Eqs. (9). The asymmetry in $\underline{H}^s(r,t)$ should not prove detrimental in performing stable numerical calculations, provided the off-diagonal level shifts and widths are not too large relative to their bound-bound counterparts V_{nm}. The asymmetry in $\underline{H}^s(r,t)$ may be aggravated somewhat at higher laser intensities I, since the level shifts and widths (as well as I) are all proportional to the *square* of the electric field amplitude E^0, whereas the bound-bound couplings V_{nm} (a.k.a. "Rabi frequencies") vary linearly with E^0. This should not be much of a problem, except perhaps at laser intensities where other approximations may have already failed.

The asymmetry in $\underline{H}^s(r,t)$ stems from using the semiclassical representation. In this representation, the field appears only as a time-dependent driving term in the total Hamiltonian, and the total system energy will not be conserved, since changes in the energy of the field are not included with those of the molecule. In the full quantum-molecule–quantum-field formulation where $\Psi(r,t)$ can be expanded in a combined molecule-field basis, one can operate within a framework whereby the total energy of the combined molecule-field system is conserved. One can then include directly in the CEH matrix only those terms that correspond to resonant bound-bound and bound-continuum transitions for which the total system energy $\varepsilon_{\text{total}}>0$ would be constant. Therefore, all relevant bound and dissociative molecule-field states would be degenerate, or nearly so,[5] *and* embedded energetically *within* the dissociative continuum, preventing any asymmetry in the resulting CEH matrix.

III. COMPARISONS BETWEEN THE BOXSW AND CEH METHODS

Using our model diatomic molecule and the Floquet theory, we will now perform some calculations comparing the CEH and BOXSW methods (see Refs. 34–36, and Secs. I and II of this work). In Sec. II, it was found that the validity of the CEH method requires that transitions between continuum states can be safely ignored, that bound-continuum couplings $V_{\varepsilon m}$ vary slowly with ε, and that time t be sufficiently long [see Eqs. (23)]. It was also argued that these conditions become more stringent as the field intensity increases. Since the original BOXSW work for this system used a field intensity of 10^{14} W/cm^2,[34] we will use this intensity as well. Such a huge intensity should help provide a "worst-case" test of the CEH method with respect to this particular factor. In comparing the CEH and BOXSW methods, attention here will be focused on how the energy dependence of the couplings $V_{\varepsilon m}$ affects the dissociation dynamics of the system. This will be done by comparing the BOXSW method, in which the bound-pseudocontinuum couplings for this system do vary strongly with energy, against the CEH method using *constant* decay widths. To test the self-consistency of the CEH formulation with constant decay widths, the original BOXSW will be modified so that the bound-pseudocontinuum couplings for the $n=3,4,5$ bound states are kept constant. The effects of the off-diagonal widths in the CEH will also be briefly examined.

To determine the energy dependence of the bound-continuum couplings for this system, the behavior of the BOXSW bound-pseudocontinuum dipole-coupling elements μ_{1n} will be examined. As discussed in Sec. I, the BOXSW pseudocontinuum states mimic, within the interval $[r=0, r=r^*]$, a subset of the true energy normalized continuum states $\chi(\varepsilon,r)$ for which $\chi(\varepsilon,r^*)=0$ (see Ref. 5, pp. 82–85, and Ref. 36). It must be remembered, however, that these BOXSW pseudocontinuum states are unit normalized within the interval $[r=0, r=r^*]$, as opposed to the energy normalizations [see Eq. (2d)] used for true continuum states. Since we are only interested in the qualitative behavior of the couplings $V_{\varepsilon m}$, the BOXSW bound-pseudoncontinuum couplings will suffice. Tabulated in Table III are the energies (real and imaginary) of the lowest 14 BOXSW pseudocontinuum states $|1\rangle$, and the relative absolute values $|\mu_{1n}|/|\mu_{6n}|$ of the bound-pseudocontinuum dipole-coupling elements μ_{1n} for the $n=3,4,5$ bound states.

Given the trends in Table III, the assumption that the couplings $V_{\varepsilon m}$ vary slowly with ε does not appear to be

TABLE III. The pseudocontinuum energies and relative bound-pseudocontinuum couplings.

l	ε_l (cm^{-1})	$\lvert\mu_{13}\rvert/\lvert\mu_{63}\rvert\times10^2$	$\lvert\mu_{14}\rvert/\lvert\mu_{64}\rvert\times10^2$	$\lvert\mu_{15}\rvert/\lvert\mu_{65}\rvert\times10^2$
6	$42-i22$	100	100	100
7	$273-i85$	88	98	106
8	$509-i160$	64	87	104
9	$731-i474$	12	16	20
10	$893-i233$	34	68	91
11	$1317-i229$	15	42	63
12	$1766-i224$	28	24	42
13	$2258-i221$	42	11	25
14	$2796-i218$	50	3	12
15	$3380-i216$	52	6	4
16	$4005-i214$	51	9	2
17	$4677-i212$	47	10	4
18	$5388-i210$	42	9	5
19	$6143-i208$	37	9	5

valid for this system. Consequently, one might not expect the CEH method to work well in this case. To test this notion, we will assume that the couplings $V_{\varepsilon m}$ are constant with ε. The results of these CEH calculations will then be compared with those of the BOXSW method. The self-consistency of the CEH using constant decay widths will also be examined using a modified version of the BOXSW. In this modified BOXSW the bound-pseudocontinuum couplings for the $n=3,4,5$ bound states will be held constant. For simplicity, a somewhat truncated form of the CEH matrix will be used by neglecting the level shifts. Some off-diagonal decay widths $\Gamma_{nm}(\varepsilon=\varepsilon_m+\hbar\omega>0)$ will also be neglected, since the BOXSW bound-pseudocontinuum couplings indicate that the couplings $V_{n\varepsilon}$ decrease rapidly for this sytem when $n<3$.

Considering the variations in the BOXSW bound-pseudocontinuum couplings, choosing constant values for μ_{13}, μ_{14}, and μ_{15} in the modified BOXSW is an arbitrary process. The same applies in choosing constant values for the CEH decay widths. The constant values of μ_{13}, μ_{14}, and μ_{15} for the modified BOXSW will be interpolated from the original BOXSW couplings at the energy $\varepsilon=\varepsilon_n+\hbar\omega$, where $\omega=2880$ cm^{-1}. If for no other reason, this field frequency was chosen since the BOXSW method was originally tested against exact finite-difference calculations at $\omega=2880$ cm^{-1}.[34] The interpolated values of μ_{14} and μ_{15} were close enough to be assigned the same constant value (in atomic units) of $-0.013-i0.002$. Since $\varepsilon=\varepsilon_n+\hbar\omega$ for the $n=3$ bound state exceeds the continuum threshold by only 7 cm^{-1} at $\omega=2880$ cm^{-1}, interpolating a constant value for μ_{13} was not so straightforward. A constant value (in atomic units) of $-0.0013-i0.0002$ was well within a reasonable range of values for μ_{13} at this energy. This value for μ_{13} is also conveniently $\frac{1}{10}$ that of μ_{14} and μ_{15}. Changing the sign of these couplings from negative to positive has only a negligible effect on the dissociation dynamics. As can be seen in Table III, the variations in the couplings μ_{1n} are also reflected somewhat by variations in the imaginary parts of the pseudocontinuum energies, particularly at lower energy. It might be argued that if the BOXSW pseudocontinuum wave functions are such that the couplings μ_{1n} are constant, then the BOXSW imaginary widths should also be fairly constant. In any case, we will include results for the modified BOXSW using both the original imaginary widths and using widths constrained to values between 208 and 233 cm^{-1}.

Due to differences in the normalization conditions, the modified BOXSW couplings μ_{1n} cannot be used directly to evaluate the diagonal and off-diagonal decay widths for the CEH. These BOXSW couplings can be used, however, to estimate the relative magnitudes of these decay widths. Since μ_{14} and μ_{15} are equal, with μ_{13} being $\frac{1}{10}$ their value, this implies $\Gamma_{55}(\varepsilon=\varepsilon_5+\hbar\omega>0)\cong\Gamma_{44}(\varepsilon=\varepsilon_4+\hbar\omega>0)$, and that $\Gamma_{33}(\varepsilon=\varepsilon_3+\hbar\omega>0)$ is about $\frac{1}{100}$ that of $\Gamma_{55}(\varepsilon=\varepsilon_5+\hbar\omega>0)$ and $\Gamma_{44}(\varepsilon=\varepsilon_4+\hbar\omega>0)$. These relative magnitudes follow from the fact that the diagonal widths are proportional to the *square* of the bound-continuum couplings. Similarly, one would expect the off-diagonal widths $\Gamma_{45}(\varepsilon=\varepsilon_5+\hbar\omega>0)$ and $\Gamma_{54}(\varepsilon=\varepsilon_4+\hbar\omega>0)$ to have about the same values as their diagonal $n=4$ and 5 counterparts. The off-diagonal widths $\Gamma_{35}(\varepsilon=\varepsilon_5+\hbar\omega>0)$, $\Gamma_{53}(\varepsilon=\varepsilon_3+\hbar\omega>0)$, $\Gamma_{34}(\varepsilon=\omega_4+\hbar\omega>0)$, and $\Gamma_{43}(\varepsilon=\varepsilon_3+\hbar\omega>0)$ are subsequently expected to be about $\frac{1}{10}$ the value of $\Gamma_{45}(\varepsilon=\varepsilon_5+\hbar\omega>0)$ and $\Gamma_{54}(\varepsilon=\varepsilon_4+\hbar\omega>0)$. Using this reasoning, the CEH decay widths for $\omega>2873$ cm^{-1} will be assigned the constant values of $\Gamma_{33}(\varepsilon=\varepsilon_3+\hbar\omega>0)=1.5$ cm^{-1}, $\Gamma_{44}(\varepsilon=\varepsilon_4+\hbar\omega>0)=\Gamma_{55}(\varepsilon=\varepsilon_5+\hbar\omega>0)=150$ cm^{-1}, $\Gamma_{45}(\varepsilon=\varepsilon_5+\hbar\omega>0)=\Gamma_{54}(\varepsilon=\varepsilon_4+\hbar\omega>0)=150$ cm^{-1}, and $\Gamma_{35}(\varepsilon=\varepsilon_5+\hbar\omega>0)=\Gamma_{53}(\varepsilon=\varepsilon_3+\hbar\omega>0)=\Gamma_{34}(\varepsilon=\varepsilon_4+\hbar\omega>0=\Gamma_{43}(\varepsilon=\varepsilon_3+\hbar\omega>0)=15$ cm^{-1}. At field frequencies less than 2873 cm^{-1} we have $\varepsilon_3+\hbar\omega<0$; therefore the widths $\Gamma_{33}(\varepsilon=\varepsilon_3+\hbar\omega>0)$, $\Gamma_{53}(\varepsilon=\varepsilon_3+\hbar\omega>0)$, and $\Gamma_{43}(\varepsilon=\varepsilon_3+\hbar\omega>0)$ are zero by definition, and the CEH matrix becomes asymmetric. The diagonal decay widths are estimated by monitoring the time-dependent decay of the system at $\omega=2880$ cm^{-1} using the modified BOXSW with constant couplings μ_{1n}. In these calculations the initial bound state $|n\rangle$ ($n=3,4,5$) was permitted to decay freely by "turning off" all couplings *except* the bound-pseudocontinuum couplings μ_{1n}. These results were then compared with the decay profile predicted by the CEH formulation in Eqs.

TABLE IV. Dissociation probability versus time from the initial $n=3$ bound state for cases A–E.

Time[a]	Case A	Case B	Case C	Case D	Case E
1τ	0.0766	0.0082	0.0081	0.0099	0.0315
2τ	0.1095	0.0351	0.0354	0.0328	0.0606
3τ	0.2090	0.0465	0.0449	0.0440	0.0852
4τ	0.3347	0.0558	0.0526	0.0508	0.1194
5τ	0.3223	0.0735	0.0677	0.0666	0.1386
6τ	0.4407	0.0863	0.0779	0.0743	0.1673
7τ	0.4568	0.0987	0.0866	0.0819	0.1835
8τ	0.5162	0.1133	0.0986	0.0920	0.2048
9τ	0.5418	0.1253	0.1061	0.1000	0.2156
10τ	0.5674	0.1343	0.1115	0.1040	0.2449
20τ	0.7364	0.2537	0.1834	0.1581	0.3743
30τ	0.7347	0.3460	0.2392	0.1956	0.4631
40τ	0.7696	0.4152	0.2873	0.2278	0.5343
50τ	0.7891	0.4729	0.3325	0.2586	0.5967
60τ	0.7980	0.5227	0.3738	0.2874	0.6479
70τ	0.8090	0.5644	0.4102	0.3137	0.6855

[a] $\tau=2\pi/\omega$, which is 487.82 atu at $\omega=2880$ cm^{-1}.

(24) for a single discrete state $|n\rangle$. These crude estimates of the constant BOXSW couplings μ_{1n} and the CEH decay widths are meant only to provide a reasonably consistent basis for *qualitative* rather that strict *quantitative* comparisons. In any case, the dissociation dynamics were found to be relatively insensitive, overall, to moderate variations in these widths and couplings. As in Ref. 34, all BOXSW calculations in this work will be performed using the lowest 14 pseudocontinuum states.

In the first set of calculations, the time-dependent profiles of the dissociation probabilities $P_n^D(t)$ from the initial bound state $|n\rangle$ ($n=3,4,5$) were evaluated at $\omega=2880$ cm^{-1} for the following cases (the values of the couplings and decay widths used in these calculations are given in the text.

Case A. The original BOXSW.

Case B. The modified BOXSW with constant bound-pseudocontinuum dipole couplings μ_{13}, μ_{14}, and μ_{15}, and the original imaginary pseudocontinuum widths.

Case C. The modified BOXSW with constant bound-pseudocontinuum dipole couplings μ_{13}, μ_{14}, and μ_{15}, and imaginary pseudocontinuum widths constrained to values between 208 and 233 cm^{-1}.

Case D. The CEH with constant diagonal and off-diagonal decay widths, and no level shifts.

Case E. The CEH with only the constant diagonal decay widths, and no level shifts.

Using Floquet theory, the dissociation probabilities $P_n^D(t)$ ($n=3,4,5$) versus time for cases $A-E$ are shown in Tables IV–VI, where $\omega=2880$ cm^{-1} and $I=10^{14}$ W/cm^2.

A cursory examination of these tables indicates that the modified BOXSW (cases B and C) and the CEH (case D) results are in much better agreement with each other than with those of the original BOXSW (case A). Except for the $n=3$ calculations, the dissociation probabilities for the two modified BOXSW methods are in good agree-

TABLE V. Dissociation probability versus time from the initial $n=4$ bound state for cases A–E.

Time[a]	Case A	Case B	Case C	Case D	Case E
1τ	0.2655	0.0704	0.0716	0.0831	0.1213
2τ	0.3953	0.1378	0.1394	0.1498	0.2257
3τ	0.5121	0.2012	0.2018	0.2243	0.3211
4τ	0.5612	0.2453	0.2455	0.2890	0.3980
5τ	0.6840	0.2761	0.2765	0.3399	0.4731
6τ	0.6854	0.3172	0.3170	0.3976	0.5290
7τ	0.7812	0.3554	0.3550	0.4452	0.5878
8τ	0.7916	0.3831	0.3819	0.4849	0.6289
9τ	0.8282	0.4152	0.4143	0.5244	0.6753
10τ	0.8645	0.4523	0.4503	0.5646	0.7052
20τ	0.9585	0.6713	0.6646	0.7865	0.8899
30τ	0.9676	0.7968	0.7869	0.8756	0.9417
40τ	0.9719	0.8680	0.8563	0.9122	0.9590
50τ	0.9741	0.9095	0.8965	0.9282	0.9675
60τ	0.9748	0.9349	0.9209	0.9362	0.9730
70τ	0.9758	0.9507	0.9361	0.9408	0.9766

[a] $\tau=2\pi/\omega$, which is 478.82 atu at $\omega=2880$ cm^{-1}.

TABLE VI. Dissociation probability versus time from the initial $n=5$ bound state for cases A–E.

Time[a]	Case A	Case B	Case C	Case D	Case E
1τ	0.2221	0.1660	0.1675	0.1919	0.1495
2τ	0.3535	0.2963	0.2967	0.3479	0.2701
3τ	0.3819	0.4479	0.4478	0.4792	0.3678
4τ	0.4280	0.5490	0.5499	0.5748	0.4514
5τ	0.5003	0.6450	0.6462	0.6523	0.5277
6τ	0.5958	0.7159	0.7170	0.7212	0.5975
7τ	0.6175	0.7714	0.7717	0.7710	0.6572
8τ	0.6747	0.8103	0.8101	0.8095	0.7046
9τ	0.7297	0.8418	0.8416	0.8437	0.7418
10τ	0.7334	0.8644	0.8645	0.8684	0.7734
20τ	0.9020	0.9626	0.9588	0.9594	0.9403
30τ	0.9558	0.9782	0.9723	0.9700	0.9749
40τ	0.9785	0.9826	0.9756	0.9722	0.9845
50τ	0.9877	0.9850	0.9776	0.9736	0.9888
60τ	0.9909	0.9871	0.9794	0.9749	0.9913
70τ	0.9928	0.9889	0.9810	0.9761	0.9931

[a] $\tau=2\pi/\omega$, which is 478.82 atu at $\omega=2880$ cm^{-1}.

ment. The differences between cases B and C in the $n=3$ results are probably due to the different imaginary widths of the lower pseudocontinuum states. These lower pseudocontinuum states are energetically accessible to the $n=3$ state by the absorption of a single photon when $2873\ \text{cm}^{-1}<\omega<3800\ \text{cm}^{-1}$. For $\omega>3800$ cm^{-1}, or so, the absorption of a single photon can excite the system from the $n=3$ state to the higher-energy pseudocontinuum states in which the imaginary widths are the same for cases B and C. The results for cases D and E indicate that the off-diagonal widths are indeed causing interference effects of some sort in the dissocation dynamics. This first series of calculations suggests that the energy dependence of the bound-continuum couplings does indeed have a considerable effect on the dissocation dynamics, which also implies that the usefulness of the CEH method for this system may be limited. Even for this huge field intensity and short time t, the CEH formulation does appear to be fairly consistent with the BOXSW systems having constant bound-pseudocontinuum couplings. Aside from the savings in computer memory, the CEH calculations also required about an order of magnitude less computation time than those using the BOXSW.

Experimentally, one might wish to determine the multiphoton dissociation yield (i.e., probability) at a given laser frequency ω, in which nearly all of the molecules are initially in the ground vibrational state. As in Ref. 34, we calculated the dissociation probability $P_n^D(t)$ (where $t=10^5$ atu and $I=10^{14}$ W/cm^2) for cases B–E as a function of field frequency ω. In these calculations the system is initially in the ground state $n=0$ at time $t=0$. The relatively short laser pulse $t=10^5$ atu was originally used in Ref. 34 in order to facilitate any subsequent classical trajectory calculations. Given that Eqs. (24) and (26) were obtained at "long time t" [see Fig. 2 with Eqs. (23)], the combination of a relatively short laser pulse and high field intensity should provide a rigrous test of the CEH method with respect to these parameters. Although the results for case A were evaluated over the frequency range 800–4000 cm^{-1},[34] cases B–E will be evaluated only from 2400 to 4000 cm^{-1}, since little dissociation activity occurs at the lower frequencies. A few calculations using the CEH were performed at some of the lower frequencies in order to detect any significant deviations from the original BOXSW results; however, none was found. The results for cases B–E will be plotted on the same frequency scale as in Ref. 34 so that direct comparisons with case A can be easily made. The laser frequencies for these calculations were selected at 2-cm^{-1} intervals such that 801 frequencies were used to evaluate $P_0^D(t)$ over the frequency interval 2400–4000 cm^{-1}.

Using the Floquet theory,[34–36,43–46,61] the time propagator matrix $\underline{U}^s(t)$ can be evaluated with particular ease if $t=p\tau$, where p is some positive integer. To take advantage of this property the time t used in these calculations for cases B–E will be set as $t=p\tau$, where $0\le(p\tau-10^5\ \text{atu})\le\tau$. Therefore, at any given ω, time t

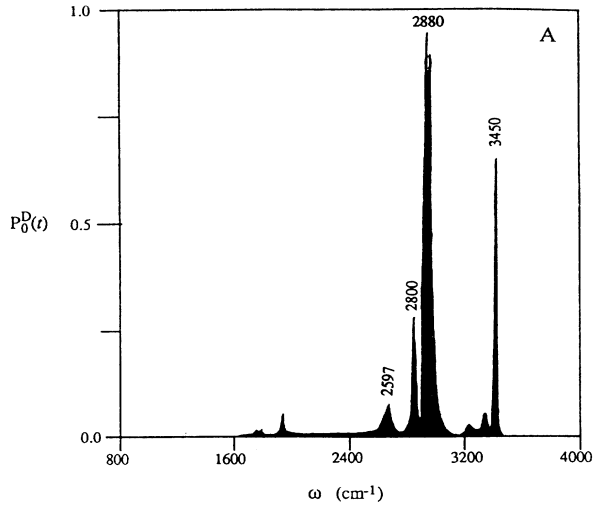

FIG. 3. The dissociation probability $P_0^D(t)$ vs ω ($800\le\omega\le4000$ cm^{-1}) for the original BOXSW (case A), where $I=10^{14}$ W/cm^2 and $t=10^5$ atu (reproduced from Ref. 34).

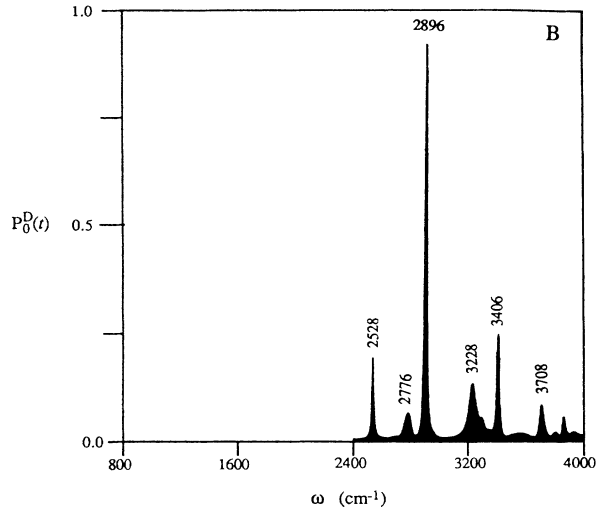

FIG. 4. The dissociation probability $P_0^D(t)$ vs ω ($2400 \leq \omega \leq 4000$ cm^{-1}) for the modified BOXSW (case B), where $I = 10^{14}$ W/cm^2 and $t \sim 10^5$ atu.

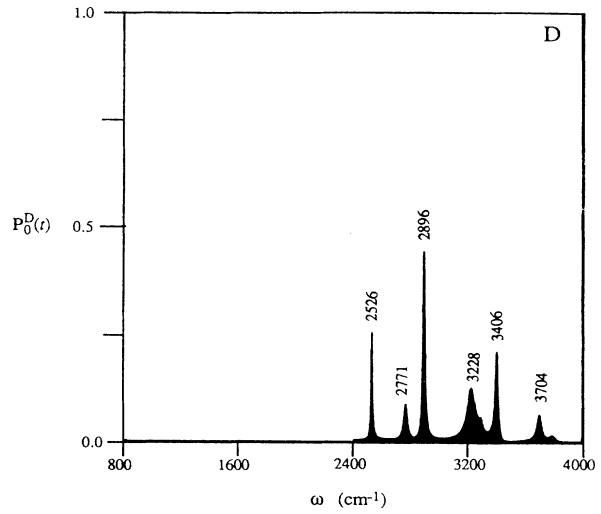

FIG. 6. The dissociation probability $P_0^D(t)$ vs ω ($2400 \leq \omega \leq 4000$ cm^{-1}) for the CEH (case D), where $I = 10^{14}$ W/cm^2 and $t \sim 10^5$ atu.

will be within one field period of 10^5 atu. These relatively small variations in time t at the various field frequencies result in only negligible differences in $P_0^D(t)$. Cases B–E will of course be consistent with each other in terms of the value of t used at a given ω. The plots of $P_0^D(t)$ versus ω for cases A–E are shown in Figs. 3–7, respectively, in which Fig. 3 was reproduced from Ref. 34. The results for cases B–E are, by far, in much closer agreement with each other than with the original BOXSW results of case A. In fact, cases B–E show very good agreement overall, especially considering the numerous assumptions and approximations that were used in these calculations. For example, due to the different normalization conditions it must be remembered that using constant values for the BOXSW bound-pseudocontinuum couplings μ_{1n} does not necessarily mean that the CEH bound-continuum couplings $V_{n\varepsilon}$ are *also strictly constant.* The CEH method also neglects the continuum-continuum couplings, and, as discussed in Sec. II, transitions between continuum states may have some influence on the dynamics at $I = 10^{14}$ W/cm^2. The differences between the original BOXSW (case A) and the modified BOXSW (cases B and C) do indicate that the energy dependence of the bound-continuum couplings can have a considerable impact on the dissociation dynamics. Even so, the major features of the original BOXSW $P_0^D(t)$ versus ω spectrum can be reproduced to a certain extent by even a rather truncated version of the CEH method.

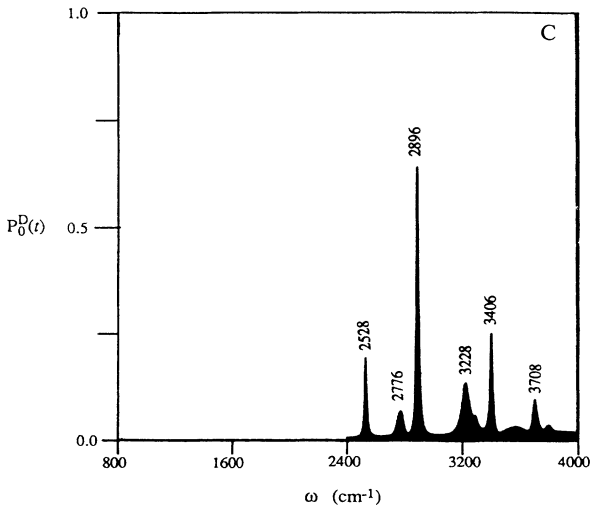

FIG. 5. The dissociation probability $P_0^D(t)$ vs ω ($2400 \leq \omega \leq 4000$ cm^{-1}) for the modified BOXSW (case C), where $I = 10^{14}$ W/cm^2 and $t \sim 10^5$ atu.

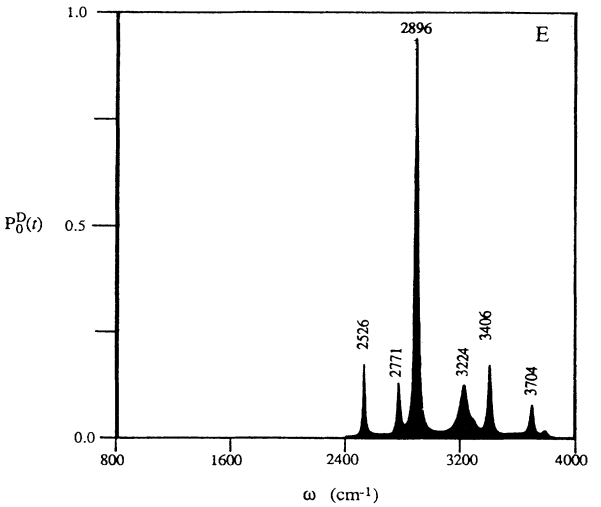

FIG. 7. The dissociation probability $P_0^D(t)$ vs ω ($2400 \leq \omega \leq 4000$ cm^{-1}) for the CEH (case E), where $I = 10^{14}$ W/cm^2 and $t \sim 10^5$ atu.

IV. SUMMARY

In this work we have formulated a complex effective Hamiltonian (CEH) approach for the study of multiphoton dissociation processes in the semiclassical (quantum-molecule–classical-field) representation. The CEH conditions of validity require that transitions between continuum states be ignored, that the bound-continuum dipole couplings be slowly varying functions of the continuum-state energy ε, and that time t be sufficiently long. These requirements are expected to become more stringent as the field intensity increases. The CEH method was applied to a model diatomic molecule that had been extensively studied previously using the BOXSW (discretized continuum plus optical potential) method.[34] Despite the huge field intensity and relatively short laser pulse, even a rather truncated CEH approach yielded very good agreement with a modified BOXSW method *provided the bound-(pseudo)continuum couplings were held effectively constant.* As might be expected, the CEH method had only limited success when compared with the original BOXSW method in which the bound-pseudocontinuum couplings did very strongly with ε. At this field intensity transitions between continuum states may also have some effect on the dynamics, which can be accounted for by the BOXSW method but *not* in the CEH approach. These results indicate that the nature of the bound-continuum dipole couplings can have a considerable effect on the dissociation dynamics, which must be kept in mind when applying any sort of CEH scheme to the study of multiphoton processes.

ACKNOWLEDGMENTS

We would like to gratefully acknowledge Dr. Claude Leforestier, Dr. Robert C. Brown, and Dr. Michael J. Davis for many useful discussions, use of the BOXSW dipole coupling data, various Floquet routines, and the Bulirsch-Stoer numerical integrator. We would also like to thank Dr. B. Ramachandran for his assistance and comments in the preparation of this manuscript. This work was supported in part by research grants from the Welch Foundation and the National Science Foundation.

[1]C. D. Cantrell, V. S. Letokhov, and A. A. Makarov, *Coherent and Nonlinear Optics: Recent Advances* (Springer-Verlag, Berlin, 1980), pp. 165–269.
[2]M. Quack, Adv. Chem. Phys. **50**, 395 (1982); and various articles in Adv. Chem. Phys. **50** (1982).
[3]N. Bloembergen and A. H. Zewail, J. Phys. Chem. **88**, 5459 (1984).
[4]C. D. Cantrell, S. M. Freud, and J. L. Lyman, in *The Laser Handbook,* edited by M. L. Stitch (North-Holland, Amsterdam, 1979), pp. 485–576.
[5]F. H. M. Faisal, *Theory of Multiphoton Processes* (Plenum, New York, 1987), and references therein.
[6]P. Lambropoulos, Adv. At. Mol. Phys. **12**, (5), 87 (1976).
[7]*Multi-Photon Excitation and Dissociation of Polyatomic Molecules,* edited by C. D. Cantrell (Springer-Verlag, Berlin, 1986) (various articles therein).
[8]Adv. Chem. Phys. **60** (1986) (various articles therein).
[9]*Laser Physics,* edited by J. D. Harvey and D. F. Walls (Academic, New York, 1980) (various articles therein).
[10]V. Weisskopf and E. Wigner, Z. Phys. **63**, 54 (1930); **65**, 18 (1930).
[11]K. O. Friedrichs, Common. Pure Appl. Math. **1**, 361 (1948).
[12]G. C. Stey and R. W. Gibberd, Physica **60**, 1 (1972).
[13]M. L. Goldberger and K. M. Watson, *Collision Theory* (Wiley, New York, 1964), Chap. 8, and references therein.
[14]E. J. Robinson, Phys. Rev. Lett. **57**, 1281 (1986).
[15]Z. Deng and J. H. Eberly, Phys. Rev. Lett. **58**, 618 (1987).
[16]M. Crance and M. Aymar, J. Phys. B **13**, L421 (1980).
[17]J. Levitan, Phys. Lett. A **129**, 267 (1988).
[18]K. Grotz and H. V. Klapdor, Phys. Rev. C **30**, 2098 (1984).
[19]C. Cohen-Tannoudji, B. Diu, and F. Laloe, *Quantum Mechanics Vol. II* (Wiley, New York, 1977), p. 1343.
[20]A. Messiah, *Quantum Mechanics* (North-Holland, Amsterdam, 1970), Chap. 21.
[21]E. Merzbacher, *Quantum Mechanics* (Wiley, New York, 1970), p. 481.
[22]M. Bixon, J. Jortner, and Y. Dothan, Mol. Phys. **17**, 109 (1969).
[23]T. D. Lee, R. Oehme, and C. N. Yang, Phys. Rev. **106**, 340 (1957).
[24]Y. Dothan and D. Horn, Phys. Rev. D **1**, 916 (1970).
[25]P. L. Knight, *Laser Physics,* edited by J. D. Harvey and D. F. Walls (Academic, New York, 1980), pp. 63–97.
[26]J. Jortner and S. Mukamel, *Excited States,* edited by E. C. Lim (Academic, New York, 1977), Vol. 3, pp. 58–107.
[27]A. Nitzan, J. Jortner, and B. J. Berne, Mol. Phys. **26**, 281 (1973).
[28]S.-I. Chu, Adv. At. Mol. Phys. **21**, 197 (1985).
[29]S.-I. Chu and W. P. Reinhardt, Phys. Rev. Lett. **39**, 1195 (1977).
[30]C. Cerjan, R. Hedges, C. Holt, W. P. Reinhardt, K. Scheibner, and J. J. Wendoloski, Int. J. Quantum Chem. **14**, 393 (1978).
[31]B. R. Junker, Adv. At. Mol. Phys. **18**, 97 (1982).
[32]K. B. Whaley and J. C. Light, J. Chem. Phys. **77**, 1818 (1982); **79**, 3604 (1983).
[33]C. Leforestier and R. E. Wyatt, Phys. Rev. A **25**, 1250 (1982).
[34]C. Leforestier and R. E. Wyatt, J. Chem. Phys. **78**, 2334 (1983).
[35]C. Leforestier and R. E. Wyatt, Chem. Phys, **98**, 123 (1985).
[36]C. Leforestier and R. E. Wyatt, J. Chem. Phys. **82**, 752 (1985).
[37]E. A. M. McCullough and R. E. Wyatt, J. Chem. Phys. **54**, 3578 (1971).
[38]R. Heather and H. Metiu, J. Chem. Phys. **88**, 5496 (1988).
[39]M. E. Goggin and P. W. Milonni, Phys. Rev. A **38**, 5174 (1988).
[40]J. R. Stine and D. W. Noid, Opt. Commun. **31**, 161 (1979).
[41]J. F. Ogilvie, W. R. Rodwell, and R. H. Tipping, J. Chem. Phys. **73**, 5221 (1980).
[42]J. F. Ogilvie, J. Phys. B **21**, 1633 (1988).
[43]S. C. Leasure and R. E. Wyatt, Opt. Eng. **19**, 46 (1980).
[44]S. C. Leasure and R. E. Wyatt, J. Chem. Phys. **73**, 4439 (1980).
[45]S. C. Leasure, K. F. Milfeld, and R. E. Wyatt, J. Chem. Phys. **74**, 6179 (1981).
[46]K. F. Milfeld and R. E. Wyatt, Phys. Rev. A **27**, 72 (1983).

[47]S.-I. Chu, J. V. Tietz and K. K. Datta, J. Chem. Phys. **77**, 2968 (1982).
[48]R. B. Walker and R. K. Preston, J. Chem. Phys. **67**, 2017 (1977).
[49]R. C. Brown and R. E. Wyatt, Phys. Rev. Lett. **57**, 1 (1986).
[50]R. C. Brown and R. E. Wyatt, J. Phys. Chem. **90**, 3590 (1986).
[51]K. M. Christoffel and J. M. Bowman, J. Phys. Chem. **85**, 2159 (1981).
[52]M. Fürisch and K. L. Kompa, J. Chem. Phys. **75**, 763 (1981).
[53]P. S. Dardi and S. K. Gray, J. Chem. Phys. **77**, 1345 (1982).
[54]M. J. Davis and R. E. Wyatt, Chem. Phys. Lett. **86**, 235 (1982).
[55]D. W. Noid and J. R. Stine, J. Chem. Phys. **76**, 4947 (1982).
[56]M. Floquet, Ann. Ec. Norm. Super. **12** (2), 47 (1883).
[57]J. H. Poincaré, *Méthodes Nouvelles de la Méchanique Céleste* (Dover, New York, 1957), Vol. I, *ibid.*; (1893), Vol. II; *ibid.* (1899), Vol. III.
[58]F. R. Moulton, *Differential Equations* (MacMillan, New York, 1930), Chap. 17.
[59]J. H. Shirley, Phys. Rev. **138**, B979 (1965).
[60]D. R. Dion and J. O. Hirschfelder, Adv. Chem. Phys. **35**, 265 (1976).
[61]W. R. Salzman, Phys. Rev. A **10**, 461 (1974).
[62]H. Sambe, Phys. Rev. A **7**, 2230 (1973).
[63]R. H. Young, W. J. Deal, Jr., and N. R. Kestner, Mol. Phys. **17**, 369 (1969).
[64]R. H. Young and W. J. Deal, Jr., J. Math. Phys. **11**, 3298 (1970).
[65]J. M. Okuniewicz, J. Math. Phys. **15**, 1587 (1974).
[66]P. K. Aravid and J. O. Hirschfelder, J. Phys. Chem. **88**, 4788 (1984).
[67]K. B. Whaley and J. C. Light, Phys. Rev. A **29**, 1188 (1984).
[68]S. L. Chin, G. Farkas, and F. Yergeau, *Coherence and Quantum Optics,* edited by Leonard Mandel and Emil Wolf (Plenum, New York, 1984), Vol. V, p. 839, discusses the ionization of Kr and Xe atoms by intense CO_2 laser pulses.